Modeling of ocean mesoscale eddy and its application in the underwater acoustic propagation

LI Jia-xun[1], ZHANG Ren[1], LIU Chen-zhao[2], FAN Hong-jun[3]

1. *PLA Research Center of Ocean Environment Numerical Simulation, Institute of Meteorology, PLA University of Science and Technology, Nanjing* 211101*, Jiangsu Province, China;*

2. *Xichang Satellite Lauch Center, Xichang* 615000*, Sichuan Province, China;*

3. *Institute of Science, PLA University of Science and Technology, Nanjing* 211101*, Jiangsu Province, China*

Abstract: Aiming at the influence of ocean mesoscale eddy on underwater acoustic propagation, a theoretical computation model of ocean mesoscale eddy was established based on the in-situ hydrographic data in the sea area of ocean mesoscale eddy. An underwater acoustic model-MMPE was used to simulate the acoustic propagation under the influence of different types, different intensities and positions of eddies, and different frequencies and depths of sources. It is found that warm-core eddy can make the convergence zone "move back" and the width of it increases, while cold-core eddy can make the convergence zone "move forward" and the width of it decreases. The bigger the intensity of eddy, the more notable the "forward "or "back "effect. Sound source located depths and source frequencies can change the acoustic propagation characteristics in the eddy area.

Keywords: MMPE model, mesoscale eddy model, transmission loss

Ocean mesoscale eddy is a rotating and moving water body which is analogous to the atmospheric vortex. Eddy has two types, that is, cold eddy and warm eddy. The former is cyclonic and the latter is anticyclonic. Usually, the typical horizontal scale of mesoscale eddy is about 50 km - 500 km, and the time scale is from about a few days to hundreds of days. Eddies have considerable kinetic energy, which is a significant peak in the ocean kinetic energy spectrum. Eddies not only affect the thermohaline structure and distribution of current speed directly, but also transport momentum and heat, and have strong impact on the physical properties of upper ocean. In this way, sound propagation of eddy area will be changed significantly. Because of the importance of underwater acoustic propagation to the sonar detection and submarine navigation, it is very significant to study the rules of the impact of ocean eddy on the underwater acoustic propagation.

Received on July 12, 2011

Corresponding author: lee_jx@126.com

When sound passes through the ocean eddies, using the non-directional 100Hz sound source, the received signal energy increases by 5% to 50% within the $\pm 5^{\circ}$ grazing angle, and different eddy locations relative to the sound source can cause about 20dB difference of transmission loss (TL)[1]. Lawrence [2] used parabolic equation (PE) method to calculate TL when sound passing through the Tasman warm eddy, and he deduced the TL function of depth and distance. Mellberg et al. [3] studied the characteristics of acoustic propagation in the Gulf Stream cold and warm core eddy area and found whether source at the eddy center or off center, and distances of the convergence zones can significantly be affected TL by using numerical simulation. Kang [4] used POM to obtain the sound speed data in the South China Sea based on multi-sources remote sensing data, and studies the impact of different types and intensities of eddy on the acoustic propagation using Gaussian eddy model. Liu [5] adopted CTD temperature and salinity data to study the structural characteristics of sound velocity field under the influence of eddies. He focused on the analysis of the mesoscale eddies on the deep sound channel, and found that the eddy has changed the nature of the surface velocity gradient (positive gradient or negative gradient), thereby affecting the appearance or disappearance of deep sound channel.

Modeling mesoscale eddy is the basement of studying the impact of mesoscale eddy on underwater acoustic propagation. According to historical hydrological data in the eddy areas, we determine the spatial scale and other parameters of eddy, and adopt a theoretical model to get the sound speed structure under the influence of the mesoscale eddies. Finally, the acoustic propagations under the influence of mesoscale eddies are simulated using the Monterey-Miami Parabolic Equation (MMPE). Before modeling the mesoscale eddies, a brief description of the mathematical theory of MMPE is necessary.

1 MMPE model

MMPE was jointly developed by Miami University and the U.S. Naval Postgraduate School [6]. It adopts parabolic equation method to solve the acoustic wave equation. Comparing with the traditional ray methods, wave number integration method and the normal mode method, MMPE model is very effective in dealing with most of the marine environment where low-frequency sound propagates long distances. It has been adopted by the U.S. Navy sonar system[7]. Considering the Helmholtz equation in three-dimensional cylindrical coordinates, the detailed model algorithm [8, 9] is as follows:

$$\frac{1}{r}\frac{\partial}{\partial r}\left(r\frac{\partial \varphi}{\partial r}\right)+\frac{1}{r^{2}}\frac{\partial^{2}\varphi}{\partial \theta^{2}}+\frac{\partial^{2}\varphi}{\partial z^{2}}+k^{2}\varphi=0 \tag{1}$$

where wave number is $k(r,z,\theta)=\omega/c(r,z,\theta)$, and ω is source frequency, and $c(r,z,\theta)$

is sound speed. Suppose the form of solution is as follows:

$$\varphi = \psi H_0^{(1)}(k_0 r) \tag{2}$$

where k_0 is reference wave number, $H_0^{(1)}(k_0 r)$ is the first kind zero rank Hankel function. After computing, we know ψ meets this differential equation:

$$\frac{\partial^2 \psi}{\partial r^2} + [\frac{1}{r} - 2k_0 \frac{H_1^{(1)}(k_0 r)}{H_0^{(1)}(k_0 r)}] \frac{\partial \psi}{\partial r} + \frac{1}{r^2} \frac{\partial^2 \psi}{\partial \theta^2} + \frac{\partial^2 \psi}{\partial z^2} + (k^2 - k_0^2)\psi = 0 \tag{3}$$

Note $k_0 r >> 1$, we choose the progressive type Hankel function and ignore the minor term, so:

$$\frac{\partial^2 \psi}{\partial r^2} + 2ik_0 \frac{\partial \psi}{\partial r} + \frac{1}{r^2} \frac{\partial^2 \psi}{\partial \theta^2} + \frac{\partial^2 \psi}{\partial z^2} + k^2 (n^2 - 1)\psi = 0 \tag{4}$$

where $n(r, z, \theta)$ is the refractive index, $n(r, z, \theta) = c_0 / c(r, z, \theta)$, and c_0 is the relative sound speed. This equation can be rewritten as:

$$\{(\frac{\partial^2}{\partial r^2} + 2ik_0 \frac{\partial}{\partial r} - k_0^2) + k_0^2 [1 + (n^2 - 1) + \frac{1}{k_0^2} \frac{\partial}{\partial z^2} + \frac{1}{k_0^2 r^2} \frac{\partial}{\partial \theta^2}]\}\psi = 0 \tag{5}$$

and

$$Z = (n^2 - 1) + \frac{1}{k_0^2} \frac{\partial^2}{\partial z^2}, \qquad Y = \frac{1}{k_0^2 r^2} \frac{\partial^2}{\partial \theta^2} \tag{6}$$

We calculate the differential operator form as the algebra variable, and divide the differential equation, so ψ satisfies:

$$(\frac{\partial}{\partial r} + ik_0 + ik_0 \sqrt{1 + Z + Y})(\frac{\partial}{\partial r} + ik_0 - ik_0 \sqrt{1 + Z + Y})\psi = 0 \tag{7}$$

The first formula represents the solution of convergence wave, and the second corresponding to divergence wave. Thus we have:

$$\frac{\partial \psi}{\partial r} + ik_0 \psi = ik_0 \sqrt{1 + Z + Y}\psi \tag{8}$$

This is the parabolic wave equation. In case the initial field is known, the numerical solution of the equation can be obtained using the "split-step Fourier algorithm".

$$\psi(r + \Delta r, z) = e^{-ik_0 \frac{\Delta r}{2} U_{op}(r + \Delta r, z)} \times FFT\{e^{-ik_0 \Delta r \hat{T}_{op}(k_z)} \times IFFT[e^{-ik_0 \frac{\Delta r}{2} U_{op}(r, z)} \times \psi(r, z)]\} \tag{9}$$

Where $U_{op} = -(n - 1)$, in the space of k_z, $\hat{T}_{op}(k_z) = 1 - [1 - (\frac{k_z}{k_0})^2]^{1/2}$.

2 Modeling of ocean mesoscale eddy

A great number of mesoscale eddies were found in the coastal waters and their

adjacent waters of China (Fig. 1), and some of them have been investigated deeply. Especially with the wide application of SSHA data from TOPEX / Poseidon (T / P) satellites, mesoscale eddy research becomes more active and positive than ever before. According to the temperature differences between ocean eddies and the surrounding waters, we can classify eddies as warm-core eddy and cold-core eddy. Eddy has a closed but irregular shape in the horizontal direction, and the profile shapes and the center positions are different in the vertical direction. Eddy can be distributed only in a single layer, and can also have distributions from the sea surface to sea bottom. Fig. 2 is the horizontal distribution of temperature and salinity plotted by Guan[11] according to the survey data from "Wings pill " research vessel from July to August, 1967. It can be seen that: At the north of Taiwan, there exists a large scale, anticyclonic warm (high temperature, low salt) eddy in oval shape. Its direction is SW-NE, with short axis of about 100 km, long axis of 150 km. While south of this eddy exists a cyclone eddy, the center temperature is about 22 °C, the temperature difference inside and outside the eddy is about 3 °C, with the short axis of about 60 km, the long axis of about 100 km.

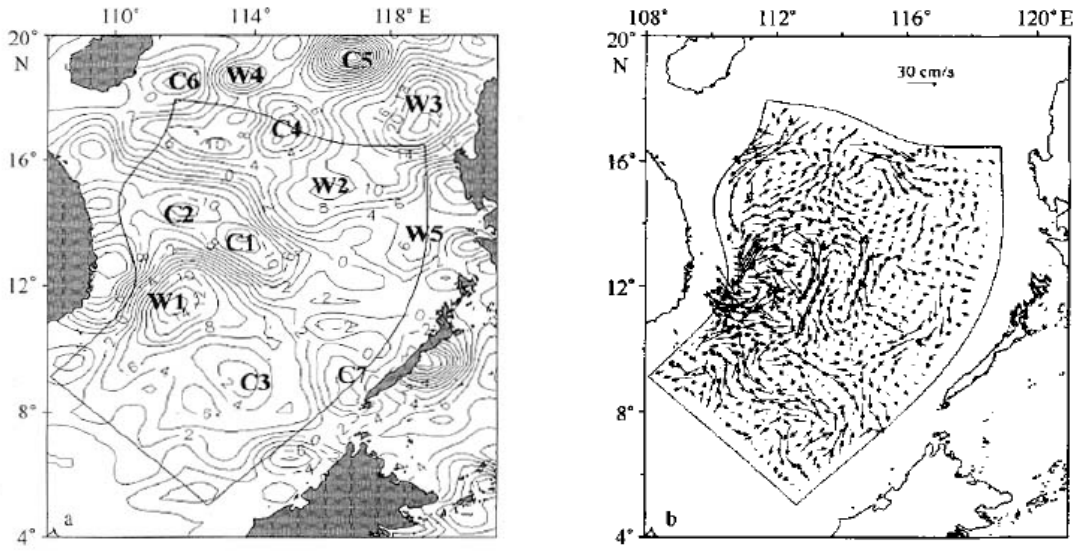

Fig. 1(a) Water level height anomaly (cm) distribution in South China Sea in August, 2008 (the data from T/P). (b) The diagnose results of SCS currents (cm/s) at the level of 200 m using an ocean model [10]

Fig. 3 shows a vertical temperature profile measured in the southern East China Sea. We can see this just corresponds to a cold eddy. The temperature of eddy core is less than 18 °C, and the temperature of eddy edge is about 29 °C, and the difference inside and outside the eddy is about 11 °C. The eddy is distributed from the surface to the bottom. Also near the 60 m depth, the isotherms are very intense, and the gradient is very large,

and this should be a thermocline, and the rapid changing structure can be found from the top to the bottom of the thermocline.

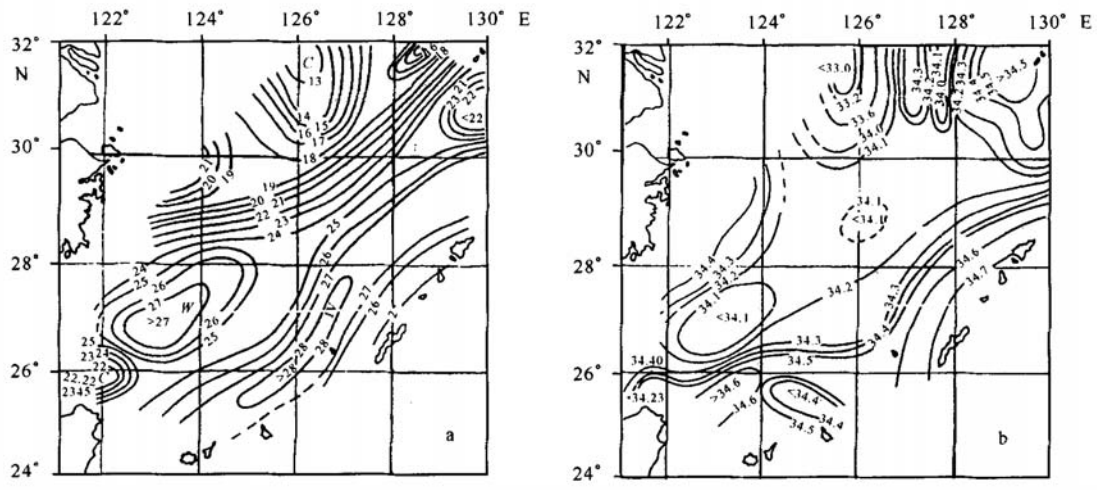

Fig. 2 Distribution of temperature (a) and salinity (b) at the level of 50 m in the East China Sea in summer, 1967 [11]

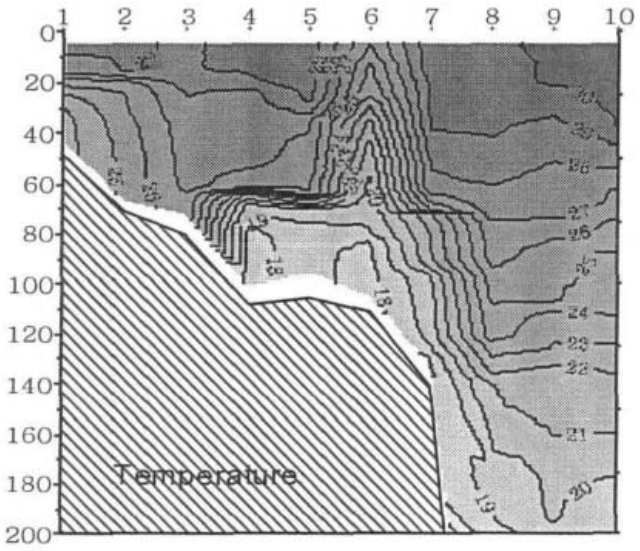

Fig. 3 An observed vertical section of temperature in the south of East China Sea [5]

Inspired by the description method of Liu[5], we first extract four characteristics of eddy: eddy center（x_0, y_0）, spatial scale（x_m, y_m）, temperature changes (core temperature T_0, and edge temperature T_1), change of depth range（$z_{\min,}\ z_{\max}$）. After the above parameters are obtained from the in-situ data, we adopt the least squares method to obtain the temperature distribution in the whole eddy area:

$$T(x,y,z)=T_0(z)+[T_1(z)-T_0(z)]r(x,y) \tag{10}$$

$$\frac{[x-x_0(z)]^2}{x_M^2(z)}+\frac{[y-y_0(z)]^2}{y_M^2(z)}=r^2(x,y) \tag{11}$$

Where $0\le r(x,y)\le 1$, $z_{\min}<z<z_{\max}$. outside the eddy $r(x,y)>1$, $T(x,y,z)$ is similar with environment temperature.

Tab. 1 Parameters adopted for the simulated cold-core eddy

Depth z	Eddy center position x_0 / m	y_0 / m	Scale in different depths x_m /m	y_m/m	Center temperature T_0 /° C	Edge temperature T_1 /° C
20	0	0	1 100	900	17	22
60	300	-400	15 000	11 000	13	18.5
120	950	-200	18 000	14 000	12	16.3
230	950	200	15 000	16 000	11.4	14
300	1 400	1 000	20 000	18 500	11	12.6
390	2 000	2 000	1 100	1 300	10.2	11

Tab. 1 shows the measured parameters extracted from the cold-core eddy. The depth of this eddy can reach 0 m - 400 m, and the biggest spatial scale is 200 km. We can see from Fig. 4 that eddy center is the minimum temperature area. In the vertical direction, the isotherms are "uplifting" distributed because of the existence of the cold eddy. Comparing with Fig. 3, general structure of our model can agree with the in-situ measured data, which validates formula (10).

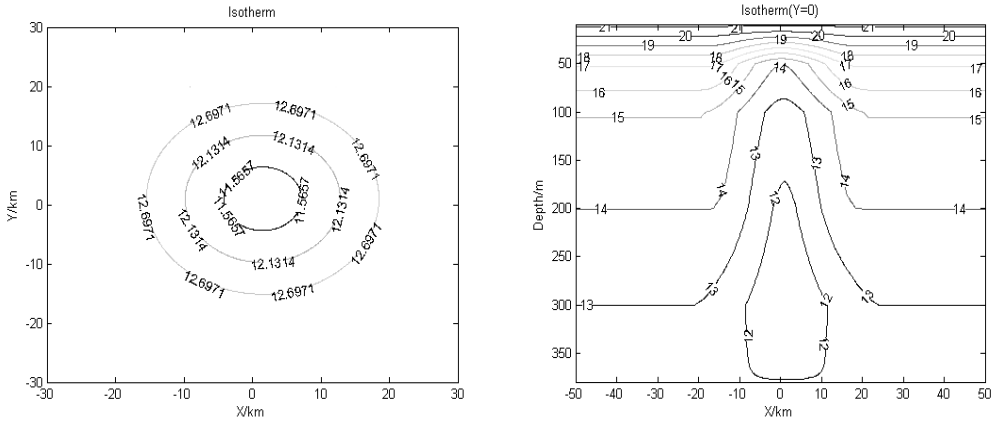

Fig. 4 Plane temperature distribution (a) at the level of 120 m and vertical temperature distribution (b) when Y=0 m in the cold-core eddy

In view of the spatial configurations and temperature structures under the influence of warm and cold eddies, Gaussian eddy model[12] is adopted to describe the ocean mesoscale eddy (Fig. 5), and acoustic propagation characteristics in the eddy area is simulated based on that model.

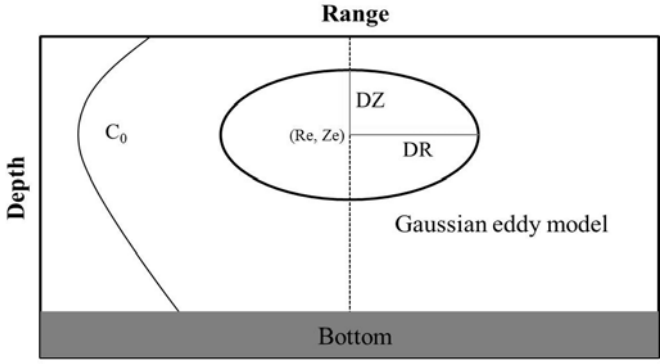

Fig. 5 Two dimensional model of Gaussian ocean eddy

Sound speed expressions of the model are as follows:

$$\left.\begin{aligned} &c(x,y,z)=c_0(z)+\delta c(x,y,z)\\ &c_0(z)=1500\{1+0.0057[e^{-\eta}-(1-\eta)]\}\\ &\delta c(x,y,z)=DC*\exp[-(\frac{r-\mathrm{Re}}{DR})^2-(\frac{Z-Ze}{DZ})^2] \end{aligned}\right\} \tag{12}$$

where $\eta=2*(z-1000)/1000$, DC is the eddy intensity, which is defined as the maximum difference between the center temperature and edge temperature. DC is negative for the cold eddy, and DC is positive for the warm eddy DR is the horizontal radius of eddy, and DZ is vertical radius of eddy, and Re is the horizontal position of eddy center, and Ze is the vertical position of eddy center.

Fig. 6 shows four pictures of sound speed contours when DC is 20, 50, -20, -50, respectively. Other parameters are $\mathrm{Re}=25km$, $Ze=400m$, $DR=20km$, $DZ=400m$. By comparison, center of warm eddy is the maximum sound speed area, and the center of cold eddy is the minimum. The bigger the eddy strength, the more intensive velocity isolines, and the bigger the velocity gradient. These validate that the Gaussian vortex model can be used to describe the ocean eddies.

3 Results and discussions

3.1 Impact analysis of different types and intensities of eddies

As for the Gaussian eddy model, four eddy intensities (DC) are taken as 20, 50, -20,

-50, respectively. Other parameters are fixed as $\mathrm{Re}=25km$, $Ze=400m$, $DR=20km$, $DZ=400m$. Source frequencies are taken as 200Hz and 1 000Hz, respectively. The depth of source is 100 m, and the relative sound speed c_0 is 1 500 m/s. The depth of the experiment area is 1000 m, and the maximum receiving range is 50 km. Bottom properties are: sound speed $c=1700m/s$, density $\rho=2.0\times10^3 kg/m^3$, and absorption coefficient 0.0.

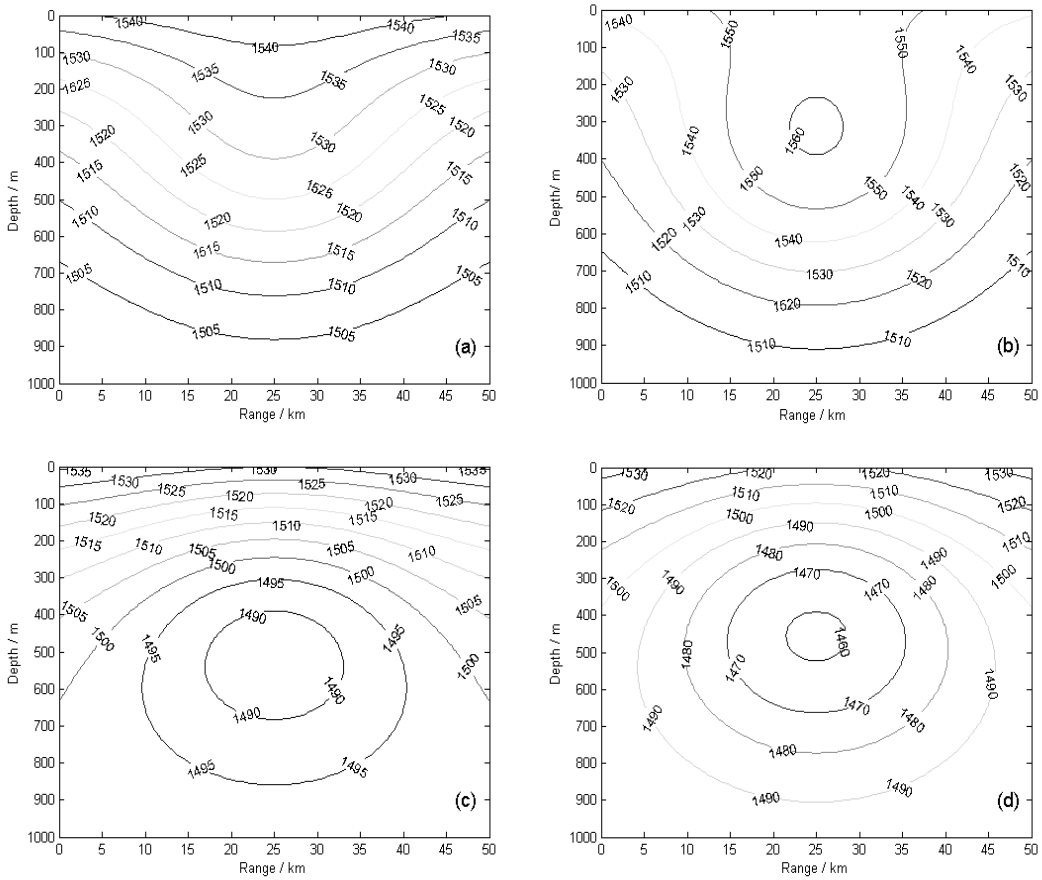

Fig. 6 Sound speed contours in different eddy intensities

((a) DC = 20, (b) DC = 50,(c) DC = -20, (d) DC = -50)

Four subplots (a-d) of Fig. 7 are TL plots of different types and intensities, and subplot (e) $DC=0$ means no eddy. TL curve comparison plots are shown in Fig. 8 when the fixed depth is 100 m. It can be seen that warm eddy makes the convergence zone back off, and the width of it increase, while cold eddy make the opposite. Taking the second convergence zone as an example, the position of second convergence zone is about 27 km, and the width is about 5 km. However, when warm eddy exists, the position is about 30 km, and the width is increased to about 8 km; when cold eddy exists, the position is about 25 km, and the width is decreased to about 3 km. The greater the intensity of eddy, the

more obvious the “back off” or “move forward” effects. The distribution of sound speed may cause this effect. The center of cold eddy is the minimum temperature area, so the times of sound wave refracting to the bottom increases, thus the convergence zone moves forward by the bottom reflection. While the center of warm eddy is in the temperature maximum area, so the times of sound wave refracting to bottom decreases, thus the convergence zone backs off by the bottom reflection.

3.2 Impact analysis of different eddy positions on acoustic propagation

The characteristic parameters of eddy are the same with the above experiment. In this experiment, we just change the positions of eddy centers: 15 km for the convergence zone and 37 km for the shadow zone.

Fig. 9 shows sound speed contours when the positions of cold eddy are different. The case of warm eddy is omitted for the limitation of article length. We can see that the positions of eddy can change the distribution of sound speed in this area, and this will affect the acoustic propagation consequently. Fig. 10(a) and (b) are TL plots when center position is 15 km in the convergence zone. When warm eddy exists, it will make the convergence zone back off and the width of convergence zone will decrease, thus convergence plus decreases. With the increasing of serial number of convergence band, the width of convergence band increases and splits obviously. When cold eddy exists, it will make the convergence zone move forward and the width will decrease, thus convergence plus increases. Fig. 10(c) and (d) are TL plots when center position is 37 km in the shadow zone. Comparing with Fig. 7(e), we find whether it is cold eddy or warm eddy, has little impact on the convergence zone when eddy center is in the shadow zone.

3.3 Impact analysis of different source frequencies and placed depths on the acoustic propagation

Fig. 11 shows TL plots when the source frequency is 1 000 Hz and the intensity of cold (warm) eddy is -50 (50). Fig. 12 is TL curve comparison plots for the source frequencies of 1000 Hz and 200 Hz, respectively. We can see from Fig. 12 that no matter the eddy is warm or cold, TL curves of high frequency and low frequency have the staggered distribution: TL curve corresponding to 1000 Hz is above that of 200 Hz in the convergence zone, while this is just converse in the shadow zone. That means high-frequency sound can strength the convergence plus in the convergence zone, while low-frequency sound can weaken the TL in the shadow zone. The mechanism needs to be further studied.

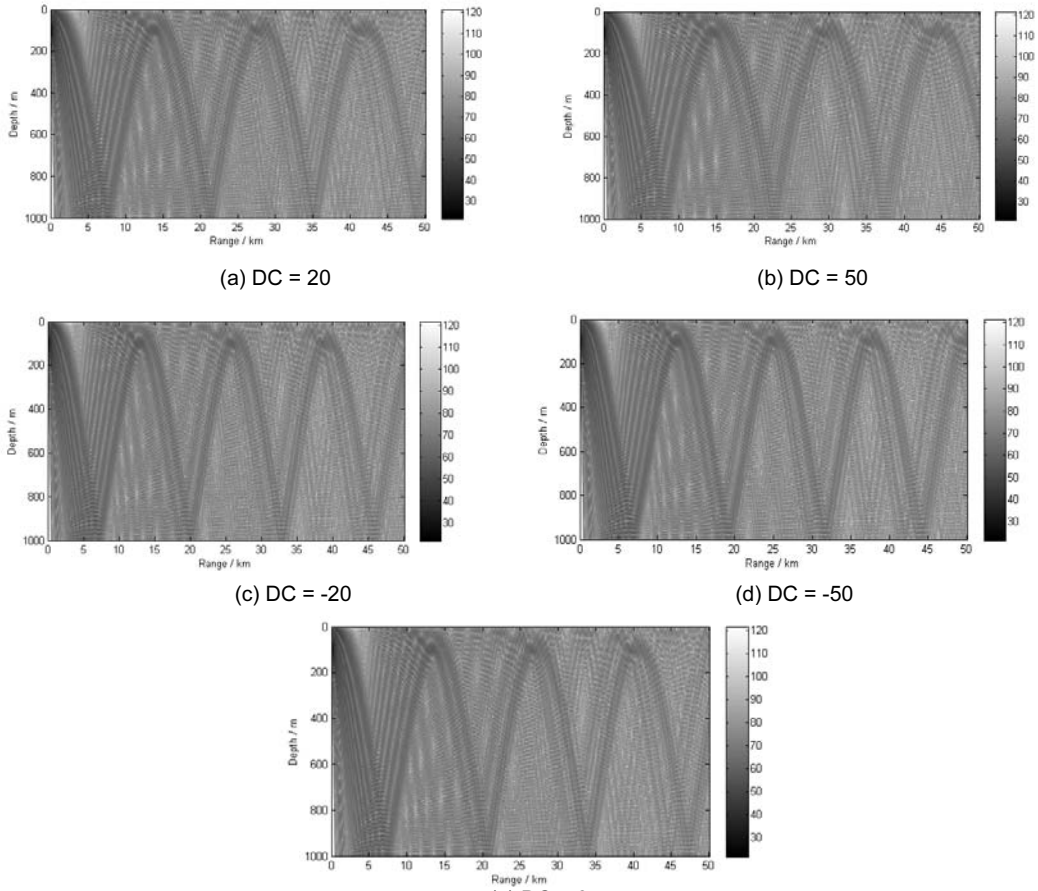

(a) DC = 20 (b) DC = 50

(c) DC = -20 (d) DC = -50

(e) DC = 0

Fig. 7 TL field changing with the depth and range (a, b represent the warm-core eddy with the intensity of 20 and 50, respectively; c, d represent the cold-core eddy with the intensity of -20 and -50, respectively;e represents no eddy)

Fig. 13 shows the TL plots of warm (left panel) and cold (right panel) eddy when source depths are fixed at 10 m, 400 m and 700 m, respectively. When the depth is 10 m (Fig. 13(a) and (b)), sound waves emitted from the source are refracted to bottom rapidly and strongly, and reflected at the range of about 5 km and continue propagating to the surface. After the reflection of sea surface, the sound energy spread to the entire space. The reason is the emergence of eddy changes the nature of surface sound velocity gradient, and the negative velocity gradient of propagation condition is formed in the range of about 5 km from the beginning point. Thus the strong refraction appears. Fig. 13(c) and (d) are the cases when the source depth is 400 m, this depth is the same with eddy center. Fig. 13(e) and (f) are the cases when the source depth is 700 m, this depth is the same with eddy bottom boundary. As for the warm eddy (Fig. 13(c) and (e)), sound waves propagate to sea surface and bottom after emitting. After continuous reflections by the

upper and lower boundary, a weak sound channel is formed in the same depth of source. As for the cold eddy (Fig. 13(d) and (f)), after several reflections by the boundaries, sound energy can converge in the lower part of cold eddy, but TL in the upper part of cold eddy is very big, and the maximum difference between two parts can be about 25 dB.

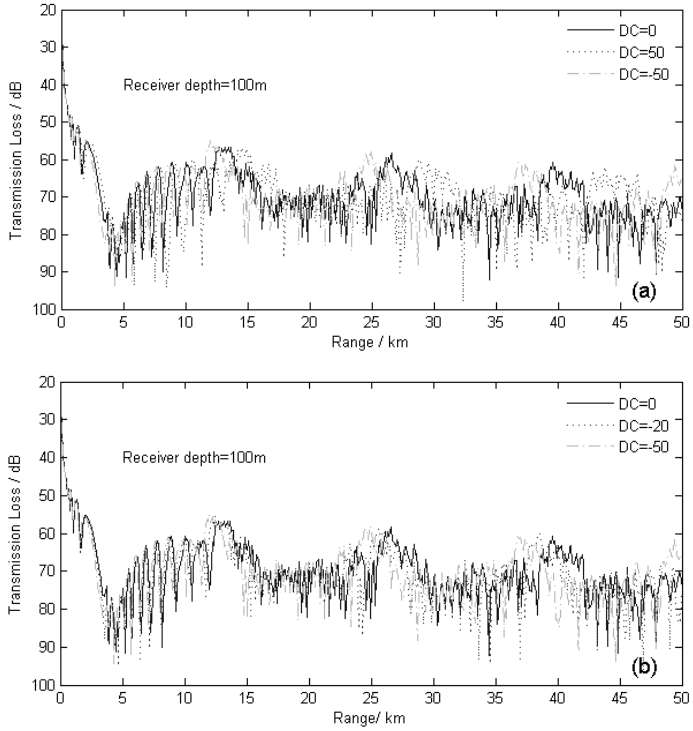

Fig. 8 Comparison of TL curves under the influence of different types (a) and intensities (b) of eddies

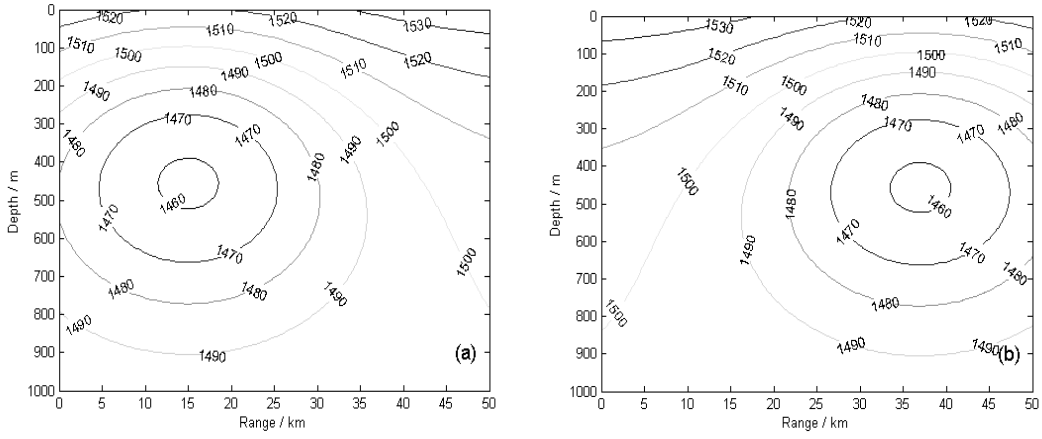

Fig. 9 Sound speed contours at the horizontal positions of 15 km (a) and 37 km (b) for cold-core eddies

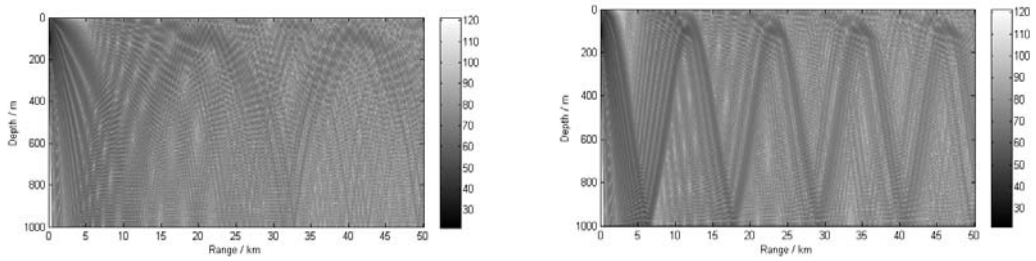

（a）range=15 km　DC=50　　（b）range=15 km　DC=-50

（c）range=37 km　DC=50　　（d）range=37 km　DC=-50

Fig. 10　Transmission loss (TL) field at different positions of eddies

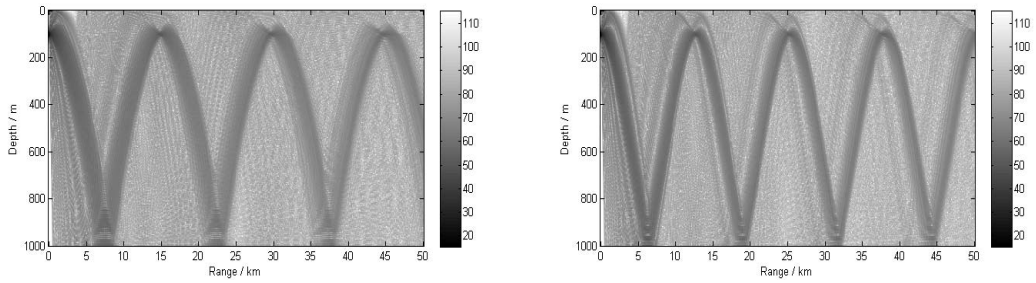

(a) f=1 000 Hz　DC=50　　**(b) f=1 000 Hz　DC=-50**

Fig. 11　TL field at different frequencies of sources (a: DC=50, b: DC=-50)

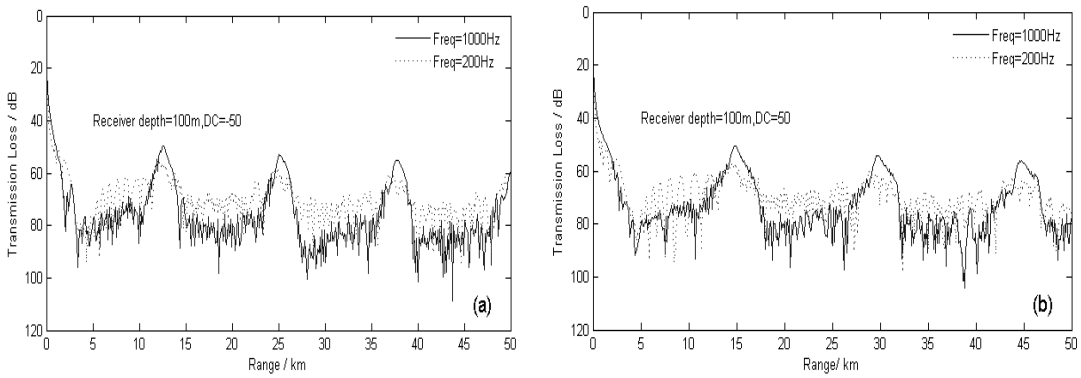

Fig. 12　Comparison of TL curves under the influence of different frequencies of sources in the cold eddy (a) and warm eddy (b)

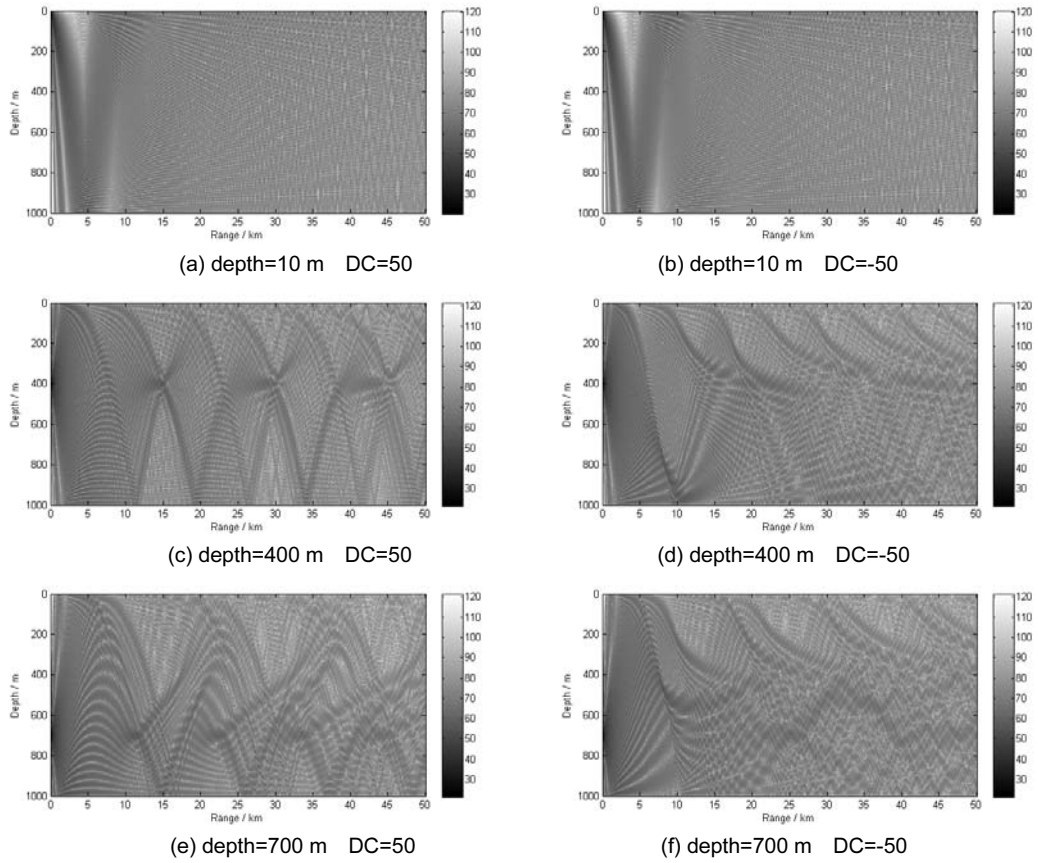

(a) depth=10 m DC=50 (b) depth=10 m DC=-50

(c) depth=400 m DC=50 (d) depth=400 m DC=-50

(e) depth=700 m DC=50 (f) depth=700 m DC=-50

Fig. 13 TL field at different depths of sources
(a and b: depth=10 m, c and d: depth=400 m, e and f: depth=700 m)

4 Summary and conclusions

According to hydrographic survey data of ocean mesoscale eddy, several characteristic parameters of ocean mesoscale eddy were extracted. Based on the Gaussian model, a theoretical model of ocean mesoscale eddies was established. Finally, MMPE was used to simulate the acoustic propagation characteristics of mesoscale eddies. Through the above study, the conclusions are as follows:

(1) The established mesoscale eddy model can represent the real conditions of mesoscale eddy comparing with in-situ data;

(2) Warm eddy makes the convergence zone "back" and the width increases, while cold eddy makes the convergence zone "forward" and the width decreases. The greater the eddy intensity, the more obvious the "forward" or "back" effects;

(3) When warm eddy is in the convergence area, it will weaken the effect of convergence plus, and will split after a certain distance transmission; when cold eddy is in the convergence area, it will enhance the convergence plus. When the eddy is in the shadow zone, no matter it is cold or warm, it will have no impact on the convergence zone.

Acknowledgments

The authors would like to express their gratitude to the National Natural Science Foundation of China (Grants No. 41176085 and 41075045), for financially supporting this research. Constructive comments by Drs. CHEN Yi-de and JIN Bao-gang are much appreciated.

Reference

[1] Baer R. Calculations of sound propagation through an eddy [J]. J.Acoust.Soc.Am., 1980,67 (4), 1 180 - 1 185.

[2] Lawrence M. Modeling of acoustic propagation across warm-core eddies [J]. J.Acoust.Soc.Am., 1983,73 (2) :474 - 485.

[3] Mellberg L, Robinson A R, Botseas G. Modeled time variability of acoustic propagation through a Gulf Stream mender and eddies [J]. J.Acoust.Soc.Am., 1990,87 (3):1 044 - 1 054 .

[4] Kang Ying. Analysis of acoustic propagation characteristics in mesoscale ocean eddies [D]. Qingdao: China Ocean University, 2004.

[5] Liu Qingyu. Sound propagation under the mesoscale ocean phenomena [D]. PhD thesis, Harbin Engineering University, 2006.

[6] Smith K B. Convergence, stability, and variability of shallow water acoustic predictions using a split-step Fourier parabolic equation model [R]. Naval Postgraduate School, 2004.

[7] Smith K B, Tappert F D. UMPE: The University of Miami Parabolic Equation Model, Version 1.0 [R]. Marine Physical Laboratory Technical Memo 432, 1993.

[8] YANG Shier. Theory of underwater acoustic propagation [M]. Harbin: Harbin Engineering University Press, 1994.

[9] Zhang Haigang. Study of acoustic computation under the marine environment with elastic seabed [D]. Harbin Engineering University, 2006.

[10] Guan Bingxian, Yuan Yaochu. Overview of studiees on some eddies in the China seas and their adjacent seas [J]. Acta Oceanologica Sinica, 2006, 28(3):1 - 16.

[11] Guan Bingxian. Main features of warm and cold eddies in the Kuroshio source region [A]. Proceedings of second China oceanography and limnology science conference. Beijing: Science Press,1983,19-30.

[12] Henrick R F. General analysis of ocean eddy effects for sound transmission application [J]. J.Acoust.Soc.Am., 1977, 62.

海洋中尺度涡建模及其在水声传播影响研究中的应用

李佳讯[1]，张 韧[1]，刘宸钊[2]，范红军[3]

（1. 解放军理工大学 气象学院 全军海洋水文环境数值模拟中心，江苏 南京 211101；
2. 西昌卫星发射中心气象室，四川 西昌 615000；3. 解放军理工大学 理学院，江苏 南京 211101）

摘 要：针对海洋中尺度涡对水声传播的影响，利用中尺度涡区的历史水文实测数据提取涡旋强度，空间尺度等中尺度涡特征参数，建立了海洋中尺度涡理论计算模型。运用MMPE水下声场模型仿真试验研究了涡旋性质、强度和位置、声源频率和置放深度对声传播特性的影响。结果表明：暖涡使得会聚区的位置“后退”，会聚区宽度增加；冷涡使得会聚区的位置“前移”，会聚区宽度减小。涡旋的强度越大，“前移”或“回退”的效应越显著。

关键词：MMPE模型；中尺度涡模型；传播损失